JOURNAL OF MATERIALS SCIENCE **40** (2005) 1647– 1654

Slow crack growth of brittle materials with exponential crack-velocity formulation—static fatigue

S. R. CHOI*, N. N. NEMETH, J. P. GYEKENYESI
National Aeronautics and Space Administration, Glenn Research Center, Cleveland, OH 44135, USA
E-mail: sung.r.choi@grc.nasa.gov

The life prediction analysis based on an exponential crack-velocity formulation was made and examined using a variety of experimental data on advanced structural ceramics in constant stress ('static fatigue' or 'stress rupture') testing at ambient and elevated temperatures. The data fit to the relation between ln (*time to failure*) versus *applied stress* was be very reasonable for most of the materials studied, resulting in a similar degree of accuracy as compared with the power-law crack-velocity formulation. The major limitation in the exponential crack-velocity formulation, however, was that the inert strength of a material must be known *priori* to evaluate the important slow-crack-growth (SCG) parameter *n*, a drawback as compared with the conventional power-law crack-velocity formulation.

1. Introduction

Advanced ceramics are candidate materials for structural applications in advanced heat engines and heat recovery systems. The major limitations of these materials in hostile environments in aeroengine applications are environmental degradation particularly for silicon-based ceramics, susceptibility to foreign object damage, slow crack growth (SCG), and creep. Slow crack growth of inherent defects or flaws generated by foreign object damage or by environmental attacks can occur until a critical size for catastrophic failure is reached. To ensure accurate life prediction of ceramic components, it is important to accurately evaluate SCG parameters of a material with specified loading and environmental conditions.

Life prediction parameters of a material depend on what type of crack-velocity formulation is used to determine them. The power-law crack-velocity formulation has been used for several decades to describe SCG behavior of a variety of brittle materials ranging from glass to glass ceramics to advanced structural ceramics [1–20]. The primary advantage of the power-law formulation over other crack-velocity formulations is the simplicity in its mathematical expression of lifetime analysis. It has also been observed that the power-law formulation has adequately described the SCG behavior of many brittle materials. Because of these merits, the power-law formulation has been used in two recent ASTM test standards [21, 22] to determine SCG parameters of advanced ceramics in constant stress-rate testing at ambient and elevated temperatures. Alternative crack-velocity formulation takes exponential forms to account for the influence of other phenomena such as corrosion reaction [23], diffusion control [24], thermal activation [25], chemical reaction with constant tip configuration [26], kinetic crack growth [27] and others [28]. However, these exponential forms, in general, do not result in simple mathematical expressions of life prediction formulation, although the forms might better represent the actual SCG behavior of some materials. Because of this mathematical inconvenience, the exponential crack-velocity formulation has rarely been used for brittle materials as a means of life prediction methodology.

In this paper, the exponential crack-velocity formulation was revisited and analyzed to achieve a more convenient and simplified life prediction under constant stress ('static fatigue' or 'stress rupture') condition through a numerical procedure. The resulting analysis obtained with the exponential formulation was compared with that of the power-law formulation to assess which would yield a better life prediction methodology in terms of accuracy and convenience. A variety of experimental data, determined in static fatigue loading for advanced structural ceramics at both ambient and elevated temperatures, were utilized for this objective. More detailed descriptions concerning the analysis and data can be found in previous reports [3, 4]. Companion papers describes the exponential crack-velocity formulations under constant stress-rate ('dynamic fatigue') [29] and cyclic fatigue [30] loading.

*Author to whom all correspondence should be addressed.

2. Theoretical background

2.1. Power-law crack-velocity formulation

The widely utilized, empirical power-law crack velocity for glasses and advanced ceramics above the fatigue limit is expressed in the following familiar form [1, 2]

$$v = \frac{da}{dt} = A\ (K_I/K_{Ic})^n \tag{1}$$

where v, a and t are crack velocity, crack size and time, respectively. K_I and K_{Ic} are mode I stress intensity factor and mode I critical stress intensity factor (or fracture toughness), respectively. A and n are called material/environment dependent SCG parameters. Constant stress ('static fatigue' or 'stress rupture') testing is performed by applying constant stress to machined test specimens to determine time to failure. The time to failure in constant stress can be analytically derived from Equation 1 to give the following familiar relation [6]:

$$t_f = D\sigma^{-n} \tag{2}$$

where t_f is time to failure, and σ is constant applied stress. The parameters D can be expressed as follows:

$$D = BS_i^{n-2} \tag{3}$$

where S_i is the inert strength whereby no SCG occurs; $B = 2K_{Ic}/[AY^2\ (n-2)]$ where Y is the crack geometry factor in the relation of $K_I = Y\sigma a^{1/2}$. The SCG parameters n and D can be obtained by a linear regression analysis with experimental data in conjunction with Equation 2. Hence, it is straightforward to determine SCG parameters n and D by least-squares fitting of the data ($\log t_f$ versus $\log \sigma$), which is the most advantageous feature of the power-law crack-velocity formulation. This convenience and merit in mathematical simplicity in addition to the use of routine test techniques have led for several decades to the almost exclusive use of the power-law crack velocity formulation in life prediction analysis and testing (in either constant stress-rate or constant stress) for many brittle materials over a wide range of temperatures.

2.2. Exponential crack-velocity formulations

Several crack-growth theories with exponential crack-velocity expression have been proposed based on other factors including chemically assisted corrosion reaction [23], diffusion-controlled stress rupture [24], thermally activated process [25], chemical reaction with constant crack-tip configuration [26], kinetic crack growth [27], and others [28]. Detailed descriptions regarding various crack growth theories are beyond the scope of the paper. The generalized exponential crack velocities in association with stress intensity factor can take following mathematical expressions:[1]

$$v = A \exp[n(K_I/K_{Ic})] \tag{4}$$

$$v = A\ (K_I/K_{Ic})\ \exp[n(K_I/K_{Ic})] \tag{5}$$

$$v = A\ (K_{Ic}/K_I)\ \exp[n(K_I/K_{Ic})] \tag{6}$$

$$v = A\ \exp[n(K_I/K_{Ic})^2] \tag{7}$$

$$v = A\ (K_I/K_{Ic})\ \exp[n(K_I/K_{Ic})^2] \tag{8}$$

where A and n are SCG parameters and are different from those used in the power-law formulation.

Unlike the power-law crack velocity formulation, the exponential crack velocity forms do not yield simple, analytical expressions of the resulting time to failure as a function of applied stress. Some attempts have been made under constant stress-rate or constant stress to obtain corresponding lifetime expressions through analytical or numerical integration [7, 26, 32, 33], incorporating in some cases with linear or nonlinear regression analysis. However, this approach still involves complexity in regression technique, as compared to the simple least-squares approach in the power-law formulation.

For the purpose of generalization, Equation 4 was chosen in this paper as a primary crack-velocity formulation. An additional analysis using other crack-velocity forms of Equations 5 to 8 was also made and the results will be discussed in the section Other Exponential Formulations. To minimize the number of parameters to be specified individually (such as $A, a, \sigma, S_i, K_{Ic}$, and t) and to accommodate more complex crack velocity formulations such as Equations 5 to 8 as well, the solution must be sought numerically.[2] Hence, for this purpose it is convenient to use a normalized scheme, as used previously for the power-law velocity formulation with complex stress intensity factor expressions [9, 17, 34]:

$$K^* = \frac{K_I}{K_{Ic}};\quad T^* = \frac{A}{a_i}t;\quad C^* = \frac{a}{a_i};\quad \sigma^* = \frac{\sigma}{S_i} \tag{9}$$

where K^*, T^*, C^*, and σ^* are, respectively, normalized stress intensity factor (SIF), normalized time, normalized crack size, and normalized applied stress. a_i is the critical crack size in the inert condition or is the initial crack size. Using these variables, the primary exponential crack-velocity equation, Equation 4, can be normalized as follows:

$$\frac{dC^*}{dT^*} = e^{nK^*} \tag{10}$$

The corresponding normalized SIF K^* in constant stress loading is expressed as

$$K^* = \sigma^*[C^*]^{1/2} \tag{11}$$

[1] Equation 4 is the form used in Refs. [23, 26]; Equation 7 in Refs. [27, 31]; Equation 8 in Ref. [28]; and Equations 5 and 6, only mathematical forms in nature, were used in Ref. [7], somewhat related to Ref. [25].

[2] The companion papers by the authors also dealt with the primary exponential crack velocity formulation as well as with more complicated equations (Equations 5–8) under constant stress-rate ("dynamic fatigue") [29] and sinusoidal fatigue ("cyclic fatigue") [30] loading conditions. Closed-form solutions can be hardly obtained in these cases so that an appropriate numerical procedure should be utilized. To be consistent in approach, the numerical procedure previously applied to dynamic and cyclic fatigue loadings was used in this paper for static fatigue. In fact, any arbitrary crack-velocity equations, regardless of complexity in loading configuration or in stress-intensity-factor expression, can be solved by the numerical analysis in conjunction with the Runge-Kutta approximation described in this section.

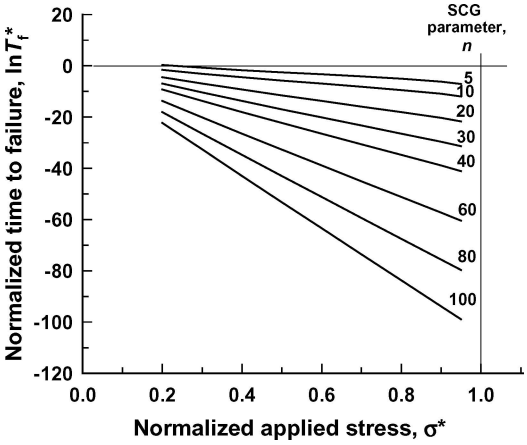

Figure 1 Numerical results of normalized time to failure T_f^* as a function of normalized applied stress σ^* in constant stress ('static fatigue' or 'stress rupture') for different values of SCG parameter n.

As typical of ceramics, the crack size at instability either in an inert or fatigue environment was assumed to be small compared with the body of the specimens or components (i.e., an infinite-body assumption). The differential equation, Equation 10, was solved by stepwise, time-incremental, numerical integration using a fourth-order Runge-Kutta method [35] starting from the initial crack size ($C^* = 0$) at $T^* = 0$ to the final crack size (C_f^*) at which the instability conditions of $K^* = 1.0$ and $dK^*/dC^* > 0$ were satisfied. At instability, the critical values such as critical crack size (C_f^*) and time to failure (T_f^*) were obtained for given n and σ^*. The numerical procedure was initiated with an input datum of n for a given applied stress (σ^*) and completed until a given range of applied stresses was covered. The procedure was repeated for other values of n. Eight different n values ranging from $n = 5$ to 100 were employed. Crack growth as a function of time from initiation ($T^* = 0$) to instability ($T^* = T_f^*$) was also obtained under any given combination of n and σ^*.

The numerical results of normalized time to failure T_f^* as a function of normalized applied stress σ^* are shown in Fig. 1, where ln T_f^* was plotted against σ^* for different n values. The general trend of the solution can be summarized in terms of the convergence of ln T_f^* close to zero with $\sigma^* \rightarrow 0$, the increased SCG susceptibility with decreasing n values, and the linearity between lnT_f^* and σ^* in the range of σ^* from 0.2 to 0.9. As a consequence, the relationship between normalized time to failure and normalized applied stress can be expressed as

$$\ln T_f^* = -n' \sigma^* + \beta \tag{12}$$

where n' is the slope and β is the intercept. The linearity between ln T_f^* and σ^* was manifest when the square of correlation coefficient of $r^2 \geq 0.995$ for each curve is considered. Hence, the slope n' and intercept β can be determined in a reasonable accuracy by a linear regression analysis of the numerical results based on Equation 12. The relationship between the slope n' and the SCG parameter n (an input datum) is shown in

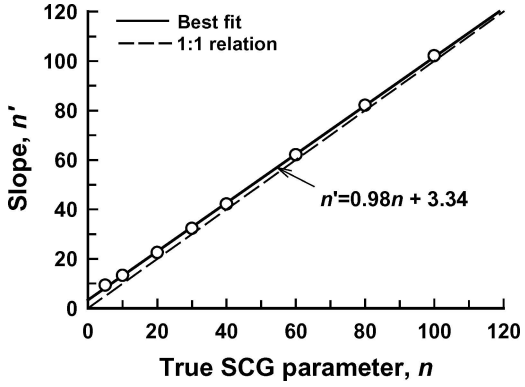

Figure 2 Relationship between SCG parameter n and n' in constant stress ('static fatigue' or 'stress rupture').

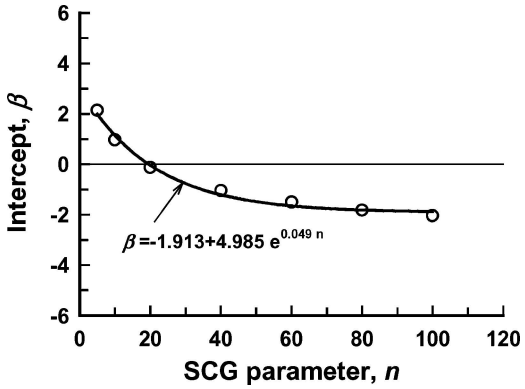

Figure 3 Relationship between intercept β and SCG parameter n in constant stress ('static fatigue' or 'stress rupture').

Fig. 2 and has the following relation:

$$n' = 0.983n + 3.344 \tag{13}$$

with $r^2 = 0.9997$. The difference between n' and n was $\geq 8\%$ for $n \leq 30$ and $n \leq 5\%$ for $n \geq 40$ so that a further approximation of Equation 13 was made for the case of $n \geq 40$ as

$$n' \approx n \tag{14}$$

The function of β with respect to n is depicted in Fig. 3, where the intercept β decreases with increasing n values, resulting in the best-fit relation

$$\beta = -1.913 + 4.985\, e^{-0.049\, n} \tag{15}$$

with $r^2 = 0.9907$.

For the non-normalized expression, Equation 9 can be used to reduce Equation 12 to

$$\ln t_f = -\frac{n'}{S_i}\sigma + \chi \tag{16}$$

where

$$\chi = \ln \frac{a_i}{A} + \beta \tag{17}$$

Therefore, n' and χ can be easily obtained from the slope and intercept, respectively, by a simple linear

TABLE I A summary of slow-crack-growth (SCG) parameters and correlation coefficients of data-fit for various brittle materials using both exponential and power-law crack-velocity formulations in constant stress loading

		Exponential formulation				Power-law formulation			
		SCG parameters				SCG parameters			
Materials	Test temp. (°C)	n	χ	A (m/s)	Corr. coeff. r^2	n	Log D	A (m/s)	Corr. coeff. r^2
Alumina [36]	RT	87.6	63.3181	5.23E-33	0.7541	54.5	126.7306	370	0.7538
Alumina (indented) [37]	RT	61.0	47.3313	1.25E-25	0.4367	39.7	86.3279	0.73	0.4411
NCX34 Si_3N_4 [38]	1200	37.3	27.4263	2.33E-17	0.8837	18.5	51.3172	2.20E-3	0.8955
NCX34 Si_3N_4 [38]	1300	36.3	22.5133	3.15E-15	0.9055	13.5	36.7292	3.37E-3	0.8988
NCX34 Si_3N_4 (tension) [38]	1200	27.0	17.5694	1.22E-12	0.6278	6.4	18.3751	1.43E-5	0.6024
NC203 SiC [39]	1300	27.6	20.2295	2.58E-14	0.3058	7.7	42.2076	1.90E-3	0.3013
Alumina [19]	1000	36.3	15.6789	5.53E-12	0.9638	15.9	20.3067	0.07	0.9798
Ceralloy 147A Si_3N_4 [40]	1200	22.9	15.5657	9.53E-12	0.6094	9.6	22.5671	3.90E-4	0.6051
Ceralloy 147A Si_3N_4 [40]	1300	38.8	17.9811	3.55E-13	0.8927	8.6	25.0071	0.02	0.8860

[1]SCG parameters n, χ and D were determined with units of time to failure in seconds and stress in MPa.
[2]Mode of tests was in four-point flexure, except for 'NCX34 (tension).'
[3]r^2 indicates square of correlation coefficient in regression.
[4]Tests at room temperature ('RT') were performed in distilled water.

regression analysis of experimental data of ln t_f as a function of σ. With n' determined from the slope and S_i, the SCG parameter n can be evaluated from Equation 13. The SCG parameter A can be estimated from Equation 17 with determined χ together with β (Equation 15) and a known value of a_i. Note that Equation 16 is significantly simpler than any other exponential solutions [7, 33]. The A notable difference in constant stress between the power-law and the exponential formulations is that in the power-law formulation, log t_f is plotted as a function of log σ as seen in Equation 2; whereas, in the exponential formulation, ln t_f is plotted as a function of σ. The knowledge of inert strength (S_i) of a material, however, is a prerequisite in determining $n$in the exponential formulation, which is not the case in the power-law formulation.

2.3. Other exponential formulations

A comparison of solutions from more complicated exponential SCG formulations is shown in Fig. 4. The figure presents the results of four exponential formulations of Equations 5 to 8 for $n = 20$ and 80 and compares them with those of the primary formulation of Equation 4. The difference in solution between the primary equation and two other first-order equations Equations 5 and 6 was insignificant, particularly at higher applied stresses, giving rise to a reasonable linearity between the dependent/independent variables related. This insignificant difference in solution as well as the linearity allows one to conclude that the primary equation would be representative of all three first-order exponential SCG formulations. By contrast, the remaining second-order formulations Equations 7 and 8 showed an appreciable deviation and a notable nonlinearity. Therefore, the determination of corresponding SCG parameters in this case differs from that of the primary equation and should only be attempted under appropriate circumstances. It is noted that the difference in solution between the two second-order formulations was negligible, implying that the order of K_I/K_{Ic} in the exponential term is indeed a key factor to affect most significantly the results of solution in constant stress, as also observed in constant stress-rate loading [29].

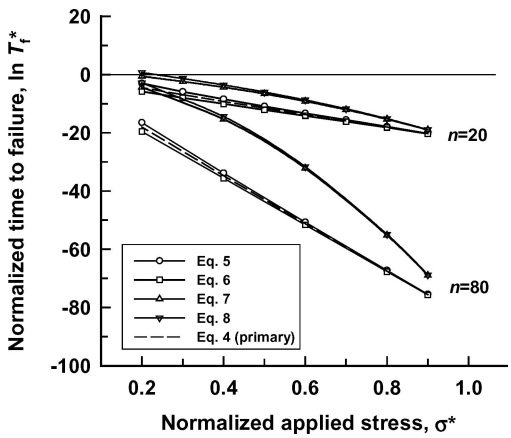

Figure 4 Results of numerical solutions using four different exponential formulations of Equations 5 to 8 compared with the primary exponential formulation of Equation 4 for selected SCG parameters of $n = 20$ and 80.

3. Experimental verification and discussion

3.1. Constant-stress tests data

The experimental data determined previously in constant stress ('static fatigue' or 'stress rupture') testing for advanced ceramics at both room (RT) and elevated temperatures were used to check the validity of the exponential SCG analysis. The advanced ceramics thus used included 96 wt% alumina [19, 36, 37], NCX34 silicon nitride (Si_3N_4) [38], NC203 silicon carbide (SiC) [39], and Ceralloy 147A silicon nitride [40] (see also Table I). Typical examples of time to failure as a function of applied stress for some of these ceramics are shown in Fig. 5, where *applied stress* was plotted against ln (*time to failure*) in accordance with Equation 16.[3] The decrease in time to failure with

[3] Time to failure is a *dependent* variable whereas applied stress is an *independent* variable; thus, ideally the resulting plots should reflect this, such as Fig 1. However, the convention is reversed such that applied stress is plotted with respect to time to failure. All figures in Figs 5 and 6 use this convention for generality.

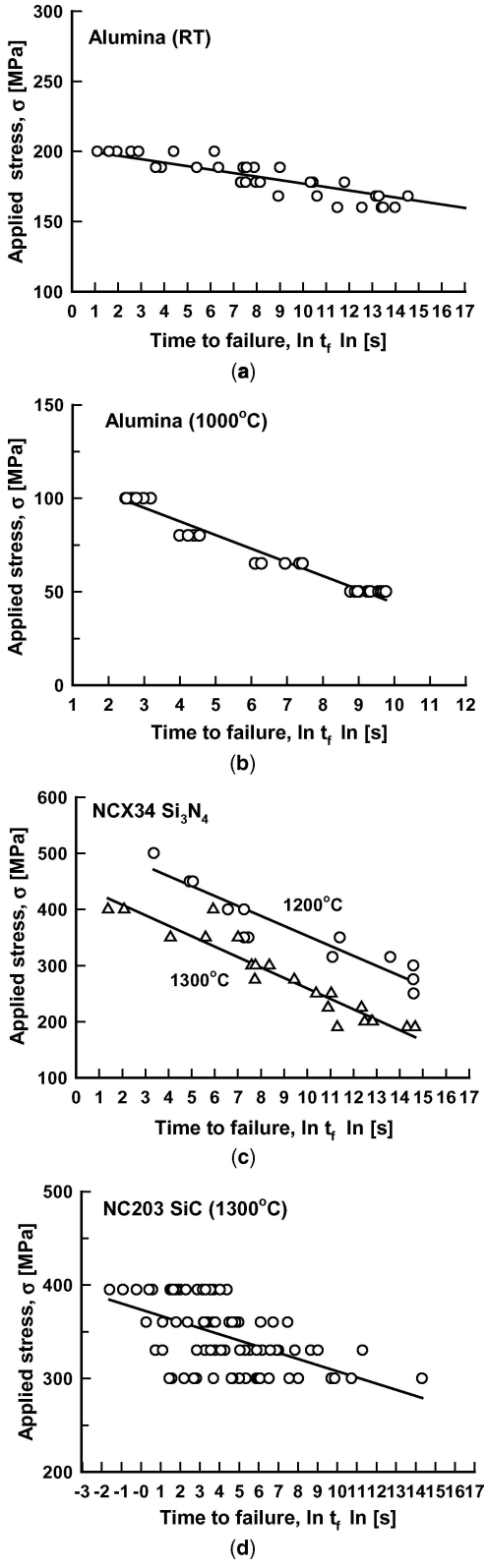

Figure 5 Ln (*time to failure* t_f) versus *applied stress* σ for some selected ceramics with the exponential crack-velocity formulation using Equation 16 under constant stress. (a) 96 wt% alumina in room-temperature (RT) distilled water in flexure [36]; (b) alumina at 1000°C in air in flexure [19]; (c) NCX 34 silicon nitride at 1200 and 1300°C in air in flexure [38]; (d) NC203 silicon carbide at 1300°C in air in flexure [39]. Solid lines represent best-fit.

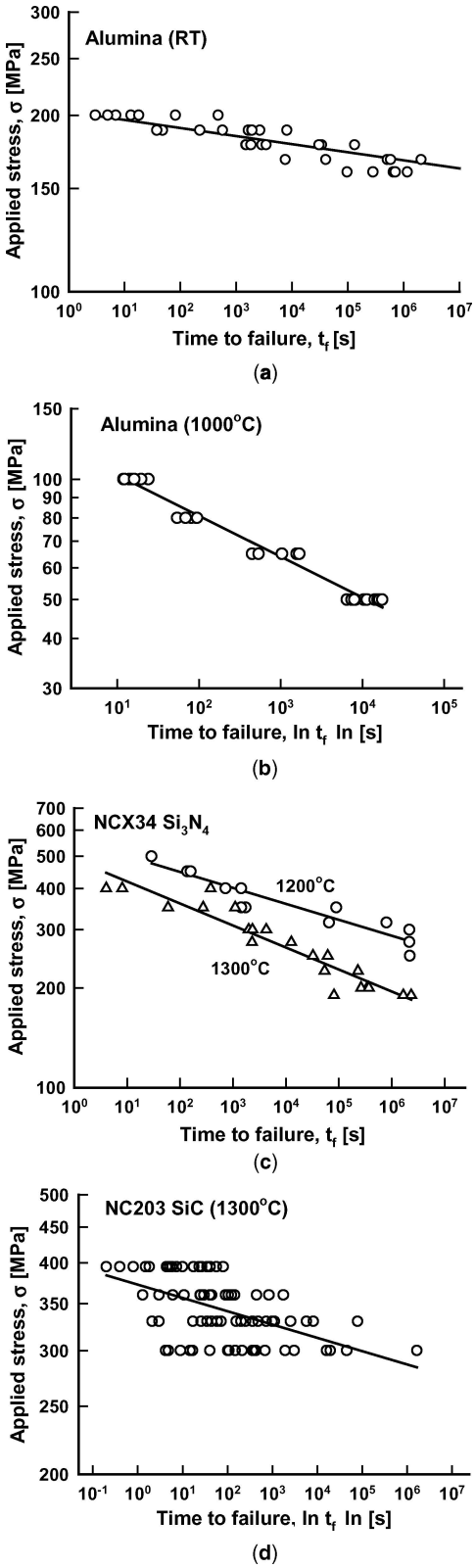

Figure 6 Ln (*time to failure* t_f) versus *applied stress* σ for some selected ceramics with the power-law crack-velocity formulation using Equation 2 under constant stress. (a) 96 wt% alumina in room-temperature (RT) distilled water in flexure [36]; (b) alumina at 1000°C in air in flexure [19]; (c) NCX 34 silicon nitride at 1200 and 1300°C in air in flexure [38]; (d) NC203 silicon carbide at 1300°C in air in flexure [39]. Solid lines represent best-fit.

increasing applied stress, which represents the susceptibility to slow crack growth, is dependent on material type and test temperature. The individual SCG parameters n and χ of each material under given test conditions were determined from the slope and intercept by the linear regression analysis of ln t_f versus σ based on Equation 16, together with inert strength [30]. The resulting SCG parameters and the correlation coefficients in regression analysis for individual materials are summarized in Table I. Fig. 6 presents the

power-law counterpart plots based on the conventional power-law relation of Equation 2. The corresponding SCG parameters n and D and the correlation coefficients for the power-law case are also listed in Table 1. Comparing the results in Figs 5 and 6 together with the correlation coefficients in Table I reveals no significant difference in data fit between the exponential and power-law formulations: The exponential formulation resulted in as good data-fit as that of the power-law formulation.

3.2. Relationship in SCG parameter n

Because of the functional form of crack velocity equation in either the exponential or power-law formulation, the SCG parameter n has the most sensitive and significant effect on lifetime; thus, accurate estimation of SCG parameter n is very important and must always be emphasized. In fact, the SCG parameter n in the conventional power-law formulation has been used as an important measure of SCG susceptibility of brittle materials: There is significant SCG susceptibility for $n < 30$, intermediate susceptibility for $n = 30$ to 50, and insignificant susceptibility (or highly resistant to SCG) for $n > 50$. Therefore, it is worthwhile to establish the relationship of n in the exponential formulation to that in the power-law formulation, which can be done using the n values from Table I. Fig. 7 illustrates the relationship between the SCG parameters from each formulation. The overall relationship was approximated as follows:

$$n_{\text{exp}} = 1.18\, n_{\text{pow}} + 18.37 \tag{18}$$

with a correlation coefficient of $r^2 = 0.9113$. The subscripts 'exp' and 'pow' denote exponential and power-law formulations, respectively. The n_{exp} is greater than n_{pow} by approximately 20. Fig. 7 also includes the relationship determined from the data in constant stress-rate testing [29], where the corresponding relationship was

$$n_{\text{exp}} = 0.96\, n_{\text{pow}} + 12.52 \tag{19}$$

with $r^2 = 0.9511$. Hence, the two relationships (Equations 18 and 19) were not in good agreement.

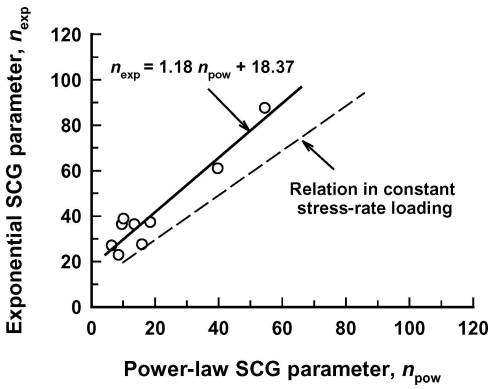

Figure 7 Relationship of SCG parameter n of exponential formulation to that of power-law for various ceramics from Table I. Relationship determined for constant stress-rate ('dynamic fatigue') loading [29] included for comparison.

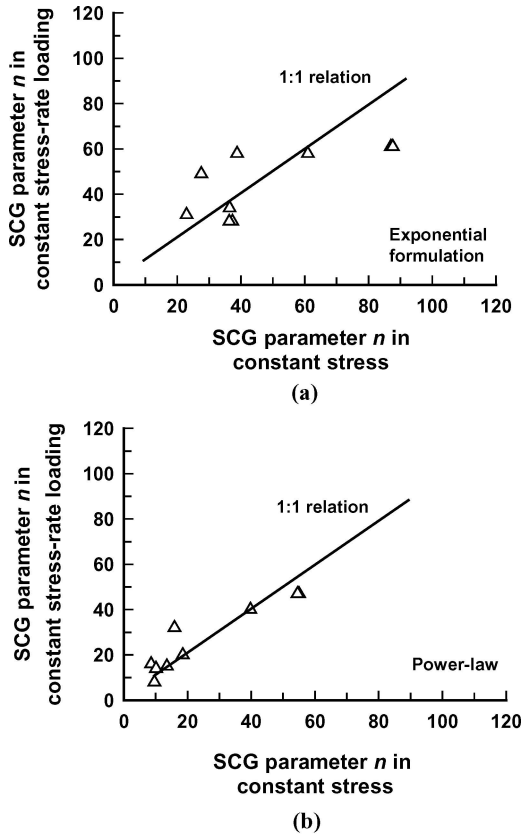

Figure 8 Relationship of SCG parameter n in constant stress-rate loading [29] and in constant stress. (a) Exponential crack-velocity formulation. (b) Power-law crack-velocity formulation.

The degree of agreement in n between the two different loadings can be seen easily if n in constant stress-rate loading [29] is plotted against that in constant stress, determined for each individual material, which is shown in Fig. 8. Although the overall relationship in n between constant stress-rate loading and constant stress seems to be 1:1 in the exponential formulation, the data scatter was significant. The corresponding relationship in the power-law formulation (Fig. 8b), however, yields good agreement between constant stress-rate loading and constant stress, which has been typical of many brittle materials observed at the NASA Glenn. The reason for less agreement in the exponential formulation is not yet clear and requires more data.

3.3. SCG parameter A and crack velocity

The parameter A can be determined using experimental data based on Equation 17, whereas the parameter A in the power-law formulation can be determined from Equation 3 with the B expression. The initial crack size or the critical crack size in the inert condition can be estimated using the fundamental relation of $K_{\text{Ic}} = Y S_{\text{i}} a_{\text{i}}^{1/2}$ together with the values of K_{Ic} and S_{i} [20, 30], assuming the crack configuration to be a semicircle ($Y = 2/\sqrt{\pi}$) and the crack size to be small compared with components or test coupons (i.e., an infinite-body approach). The resulting A parameters for each material thus estimated for both the exponential and power-law formulations are also shown in Table I. Unlike SCG parameter n, no definite relationship existed for A between the two formulations, which

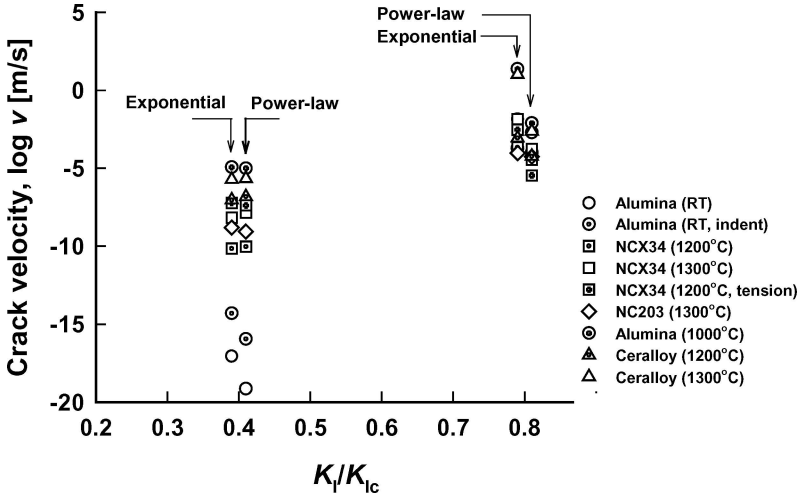

Figure 9 Comparison of crack velocity as a function of stress intensity factor (K_I/K_{Ic}) in both the exponential and the power-law formulations for the ceramic materials used in this work.

was similar to that observed in constant stress-rate loading [29]. Notwithstanding, the actual crack velocities for a given stress intensity factor seem not much different from each other with some exceptions, as can be seen from the results of log v vs. K_I/K_{Ic} in Fig. 9.

3.4. Limitation of exponential formulations

Although the exponential formulations used to determine SCG parameters required somewhat inconvenient numerical procedures, their resulting simplified solutions under constant stress showed to yield almost the same degree of simplicity in data analysis as well as in the agreement in experimental data as those in the power-law formulation. The same was observed to be true for constant stress-rate loading condition, as appeared from the previous results [29]. However, that inert strength of a material must be known in advance to determine the *major* SCG parameter n can be a drawback in using the exponential formulation in terms of simplicity and accuracy, as compared with the power-law counterpart that does not require knowledge of the inert strength. Inert strength of a material at room temperature, of course, is not difficult to determine; however, even in this case care must be exercised to provide a perfect inert condition by using an appropriate conditions (environment and test rate) so that an accurate inert strength can be evaluated. A greater burden would be determining inert strength at elevated temperatures, although the authors have done a pioneering work in this subject using a total 17 advanced ceramics [20] with some conclusive results that the elevated-temperature inert strength of a ceramic material can be estimated with a *ultra-fast* test rate of $\geq 10^5$ MPa/s and that the elevated-temperature inert strength is close to that of the room-temperature. However, to get another SCG parameter A, inert strength is equally needed either in the exponential formulation or in the power-law counterpart.

4. Conclusions

1. The data fit to the ln (*time to failure*)-versus-*applied stress* relation numerically solved in the exponential crack-velocity formulation was found very reasonable for most of the advanced ceramics used.

2. A reasonable relationship of slow-crack-growth (SCG) parameter n existed under 'static fatigue' loading, determined with the exponential formulation to those determined with the power-law formulation. However, this relationship was not similar to those determined under constant stress-rate loading.

3. Despite little difference in the data fit, the major limitation in the requirement of knowledge of inert strength in evaluating the *major* SCG parameter n makes the power-law formulation a more preferable choice for life prediction than the exponential formulation. Also, the exponential approach would require in many cases an inconvenient numerical analysis even when a slight change in loading from static to time-varying configuration occurs.

Acknowledgements

This work was sponsored in part by Higher-Operating Temperature Propulsion Components (HOTPC) Program, NASA Glenn Research Center, Cleveland, Ohio.

References

1. A. G. EVANS, *Int. J. Fracture* **10**(2) (1974) 251.
2. S. M. WIEDERHORN, in "Fracture Mechanics of Ceramics," edited by R. C. Bradt, D. P. H. Hasselman and F. F. Lange (Plenum Press, New York, NY, 1974) Vol. 2, p. 613.
3. A. G. EVANS and E. R. FULLER, *Metall. Trans.* **5**(1) (1974) 27.
4. D. G. MILLER, C. A. ANDERSON, S. C. SINGHAL, F. F. LANGE, E. S. DIAZ and R. KOSSOWSKY, "AMMRC CTR 76-32, Army Materials & Mechanics Research Center" (Watertown, MA, 1976).
5. T. T. WANG and H. M. ZUPKO, *J. Mater. Sci.* **13** (1978) 2241.
6. J. E. RITTER, in "Fracture Mechanics of Ceramics," edited by R. C. Bradt, D. P. H. Hasselman and F. F. Lange (Plenum Press, New York, NY, 1978) Vol. 4, p. 661.
7. G. G. TRANTINA, *J. Am. Ceram. Soc.* **62**(7/8) (1979) 377.
8. K. JAKUS, T. SERVICE and J. E. RITTER, *ibid.* **63** (1980) 4.
9. B. R. LAWN, D. B. MARSHALL, G. R. ANSTIS and T. P. DABBS, *J. Mater. Sci.* **16** (1981) 2846.
10. S. SAKAGUCHI and T. KIMURA, *J. Am. Ceram. Soc.* **64**(5) (1981) 259.

11. P. W. FRANCE, W. J. DUNCAN, D. J. SMITH and K. J. BEALES, *J. Mater. Sci*. **18** (1983) 785.
12. G. QUINN and J. B. QUINN, in "Fracture Mechanics of Ceramics," edited by R. C. Bradt, A. G. Evans, D. P. H. Hasselman and F. F. Lange (Plenum Publishing Corp., New York, NY, 1983) Vol. 6, p. 603.
13. T.-S. WEI, *Adv. Ceram. Mater*. **1**(3) (1986) 237.
14. P. K. KHANDELWAL, J. CHANG and P. W. HEITMAN, in "Fracture Mechanics of Ceramics," edited by R. C. Bradt, A. G. Evans, D. P. H. Hasselman and F. F. Lange (Plenum Press, New York, NY, 1986) Vol. 8, p. 351.
15. M. H. RAWLINS, T. A. NOLAN, L. F. ALLARD and V. J. TENNERY, *J. Am. Ceram. Soc.* **72** (1989) 1338.
16. Y. TAJIMA, K. URASHIMA, M. WATANABE and Y. MATSUO, in "Ceramic Materials Components for Engines," edited by V. J. Tennery (The American Ceramic Society, Westerville, OH, 1989) p. 719.
17. S. R. CHOI, J. E. RITTER and K. JAKUS, *J. Am. Ceram. Soc*. **72** (1990) 268.
18. N. L. HECHT, in "Ceramic Technology Project," Semiannual Progress Report for 10/1992 to 3/1993, ORNL/TM-12428, Oak Ridge National Laboratory, Oak Ridge, TN (1993), p. 329.
19. S. R. CHOI and J. P. GYEKENYESI, *ASME J. Eng. Gas Turb. Power* **123** (2001) 277.
20. *Idem.*, in "Fracture Mechanics of Ceramics," edited by R. C. Bradt, D. Munz, M. Sakai, V. Shevchenko and K. W. White (Kluwer Academic/Plenum Publishers, New York, NY, 2002) Vol. 13, p. 27.
21. ASTM C 1368, "Annual Book of ASTM Standards Vol.15.01," (American Society for Testing & Materials, West Conshohocken, PA, 2004).
22. ASTM C 1465, "Annual Book of ASTM Standards Vol.15.01," (American Society for Testing & Materials, West Conshohocken, PA, 2004).
23. W. S. HILLIG and R. J. CHARLES, in "High Strength Materials," edited by V. F. Zackay (Wiley & Sons, New York, NY, 1965) p. 682.
24. R. J. CHARLES, *Metall Trans*. **A7** (1976) 1081.
25. J. C. POLLET and S. J. BURNS, *Int. J. Fract*. **13**(5) (1977) 667.
26. S. M. WIEDERHORN and L. H. BOLZ, *J. Am. Ceram. Soc*. **53** (1970) 543.
27. B. R. LAWN, *J. Mater. Sci*. **10** (1975) 469.
28. E. M. LENOE and D. M. NEIL, AMMRC TR 75-13, ARPA Order No. 2181 (1975).
29. S. R. CHOI, N. N. NEMETH and J. P. GYEKENYESI, in print, Fat. & Fract. Engr. Mater (2004). Also in *NASA/TM*-2002211153/PART2, National Aeronautics & Space Administration, Glenn Research Center, Cleveland, OH (2002).
30. *Idem.*, *NASA/TM*-2002-211153/PART3, National Aeronautics & Space Administration, Glenn Research Center, Cleveland, OH (2002).
31. B. J. S. WILKINS and R. DUTTON, *J. Am. Ceram. Soc*. **59**(3/4) (1976) 108.
32. J. E. RITTER, M. VICEDOMINE, K. BREDER and K. JAKUS, *ibid.* **67** (1984) C-198.
33. J. E. RITTER, K. JAKUS and D. S. COOKE, in Proc. Second International Conference on Environmental Degradation of Engineering Materials, edited M. R. Louthan, R. P. McNitt and R. D. Sisson (Virginia Polytechnique Institute, 1981), p. 565.
34. S. R. CHOI and J. P. GYEKENYESI, *J. Mater. Sci.* **34** (1999) 3875.
35. See any texts such as C. G. Gerald, "Applied Numerical Analysis," (Addison-Wesley Publishing Company, New York, NY, 1980) Chapt. 5.
36. S. R. CHOI, unpublished work, National Aeronautics & Space Administration, Glenn Research Center, Cleveland, OH (1991, 2000).
37. S. R. CHOI and J. A. SALEM, *J. Mater. Sci. Lett*. **14** (1995) 1286.
38. S. R. CHOI, J. A. SALEM and J. L. PALKO, in "Life Prediction Methodologies and Data for Ceramic Materials. ASTM STP 1201," edited by C. R. Brinkman and S. F. Duffy (American Society for Testing & Materials, Philadelphia, PA, 1994) p. 98.
39. S. R. CHOI and N. N. NEMETH, *J. Mater. Sci*. **33** (1998) 1325.
40. S. R. CHOI, unpublished work, National Aeronautics & Space Administration, Glenn Research Center, Cleveland, OH (1991).

Received 22 January
and accepted 19 October 2004